IEEE Access
Multidisciplinary | Rapid Review | Open Access Journal

Received May 28, 2019, accepted August 7, 2019, date of publication September 3, 2019, date of current version June 19, 2020.

Digital Object Identifier 10.1109/ACCESS.2019.2939277

Research on the Thermal-Electric Coupling Behavior Under Compound AC-DC Voltage Within Saddle-Like Electric-Stress Dependence

DUAN PAN[1], (Member, IEEE), GAO BING[2], CHI CHENG[2], YANG FAN[2], (Member, IEEE), AND LUO PING[1]

[1]School of Automation, Chongqing University of Posts and Telecommunications, Chongqing 400065, China
[2]State Key Laboratory of Power Transmission Equipment and System Security and New Technology, School of Electrical Engineering, Chongqing University, Chongqing 400044, China

Corresponding author: Duan Pan (duanpan@cqupt.edu.cn)

This work was supported in part by the National Natural Science Foundation of China under Grant 51807018, in part by the National Natural Science Foundation of China (Key Program) under Grant 51837002, and in part by the Chongqing Postdoctoral Research Project under Grant Xm2017195.

ABSTRACT This paper proposes a nonlinear electromagnetic-thermal-velocity coupling model to study the insulation performance of converter transformer, in which the saddle-like electric-stress dependence is considered under compound alternating current–direct current (AC-DC) voltage situation. Firstly, the conductance of transformer oil and oil-immersed pressboard have been measured through constructed three-electrode experimental system. An interesting electric-stress characteristic, which is saddle-like electric-stress dependence is obtained and counted in the thermal-insulation analysis in the proposed model. Then, the high-order harmonics of compound AC-DC voltage have been considered in the built electromagnetic-thermal-velocity coupling model. Additionally, the impact of non-uniform temperature result has been mapped to the electric field domain through interpolation method, due to different meshes between the flow-thermal and electric fields in accordance with distinct computational characteristics. Finally, the performance of nonlinear thermal-electric coupling properties, including saddle-like electric-stress dependence, have been considered in the proposed coupling model. Results determine that saddle-like thermal-electric dependent properties would considerably change insulation capability, compared with results from the traditional method. Even intensity field of some sampling points could jump more than 1.6 kV/mm. Therefore, it is essential to evaluate the insulation design by practical saddle-like electric-dependent properties.

INDEX TERMS Compound ac–dc voltage, converter transformer, electric-stress dependence, finite element sub-model, electromagnetic-thermal-velocity coupling.

I. INTRODUCTION

Converter transformer in high voltage direct current (HVDC) system is one of the most significant equipment for ensuring electric network security, and its operation condition is different from that of the traditional transformer. Specifically, the direct current (DC) component and high-order harmonic current of voltage source have a great influence on insulation state and thermal condition, respectively. In reality, the valve winding has to suffer a compound alternating current–direct current (AC-DC) voltage, which includes a DC voltage component, fundamental sinusoidal voltage, and high-order harmonics. This hybrid-exciting source generates a resistive and capacitive electric field [1]; however, the production test, such as DC or polarity reversal test, cannot archive to predict the compound field.

Under the compound AC-DC condition of converter transformer, the coupling phenomenon is severe due to larger temperature and electric field. Recent studies show that insulation conditions of transformer oil and oil-immersed pressboard (PB) can be easily affected by field intensity [2], temperature [3], moisture [4], and mechanical stress, and the conductivity of insulation materials markedly increases with the temperature [5]. Therefore, thermal study is an important part in coupling analysis, which would greatly affect the electric filed distribution. Scholars have also conducted thermal

The associate editor coordinating the review of this manuscript and approving it for publication was Guiwu Wei.

research of converter transformer. Reference [6] stated that the highest temperature is approximately 50 K higher than the ambient temperature and the hot spot is located near the top of line winding. Reference [8], [9] considered non-uniform losses in analyzing temperature distribution, and demonstrated that high-order harmonic, which could enlarge losses, should be considered.

Additionally, field intensity would also have influence on conductance, and the latest report of CIGRE joint working group [10] demonstrated that the trend curve of oil electric-dependent conductivity is saddle-like, which is different from the traditional exponential manner [11]. However, in previous studies, the electric-stress dependence has been ignored or assumed as an exponential relationship for designing the insulation margin, which would deviate from the actual operation condition, leading to safety hazard.

In this paper, an electromagnetic-thermal-velocity coupling model is constructed on the basis of the measured insulation properties to test nonlinear thermal-electric coupling behavior within the saddle-like electric-stress dependence. The three-electrode experimental platform is constructed to test the electro-thermal coupling characteristic and electric-stress dependence in Section II. Section III describes the coupling model in considering of the high order harmonic and the impact of non-uniform temperature distribution through the proposed fast mapping method. Section IV depicts the entire model and sub-model, which are utilized in temperature and electric field, respectively, and discusses the boundary conditions and meshing information in detail. Section V studies the effect of saddle-like electric-stress dependence on nonlinear thermal-electric performance of converter transformer. Finally, Section VI concludes the entire work.

II. MEASURING SYSTEM AND EXPERIMENTAL DATA

A. THERE-ELECTRODE SYSTEM

This study adopted a three-electrode method [12] with higher accuracy to test the physical parameter of transformer oil and oil-immersed pressboard. The experimental platform is shown in Fig.1, and the test cell consists of high-voltage, guard, and test electrodes. A high voltage can provide a DC voltage from 0.1 kV to 20 kV, and measuring electrode connects with Keithley electrometer. Besides, all electrodes are designed according to the national standard to diminish electric field distortion, and the electrode system sets in the PTFE tank achieves a uniform temperature from 273 K to 393 K in the thermostat. The conductivity should be obtained on the basis of the structure and size of the electrode, as follows:

$$\sigma_V = \frac{1}{R} \times \frac{h}{A}, \tag{1}$$

where V is the volume conductivity (S/m), due to the leakage current going through the insulation material; R is the measured volume resistance (Ω) when the measuring current is stable; A is the effective area of the measuring electrode (m^2), which can be calculated on the basis of the national standard [13]; and h is the sample thickness (m), which is equal to the electrode gap when the transformer oil is measured.

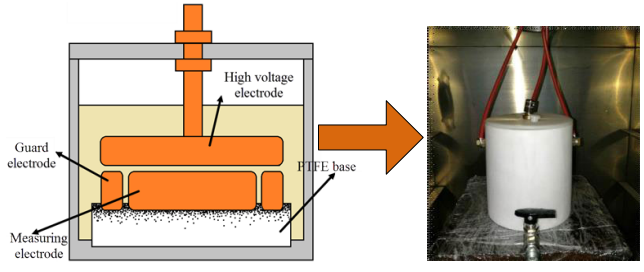

FIGURE 1. Schematic of the three-electro system.

B. CONDUCTIVITY MEASURED RESULTS

The KI50X mineral oil produced by Kunlun Lubricant, which is widely utilized in HVDC project, has been selected as the oil sample after filter and heat. The measured temperature ranges from 300 K to 360 K under an electric field ranging from 0.1 kV/mm to 15 kV/mm. Fig.2 shows that the conductivity increases with the temperature at a slope of 11.5×10^{-13}. The changing tendency of electric-stress dependence is saddle-like, and the knee point is approximately 2 kV/mm. This variation is different from the traditional exponential manner, but it accords well with the latest report from the CIRGRE joint working group. The saddle-like tendency greatly affects the electric field, which may mislead the previous insulation evaluation and cause potential hazard.

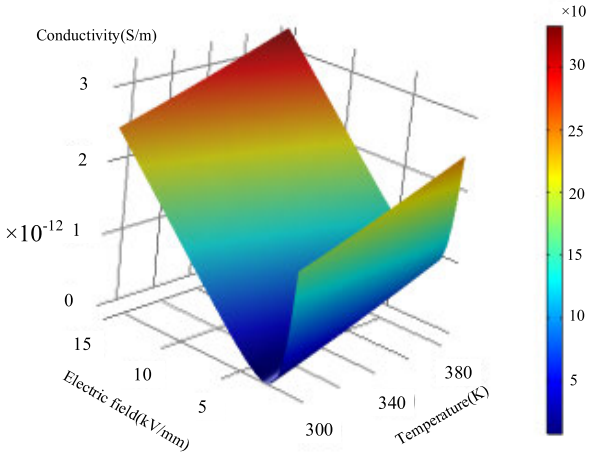

FIGURE 2. Thermal–electric relationship of transformer oil.

The adopted transformer-board type is T4, which is provided by Weidman Company Ltd., and it should be pretreated on the basis of the national standard before measurement. Fig. 3 demonstrates the relationship of temperature and electric field. It shows that when the electric field ranges from 0.1 kV/mm to 10kV/mm, the conductivity rises more than twice of initial value, and the conductivity fluctuation is lower

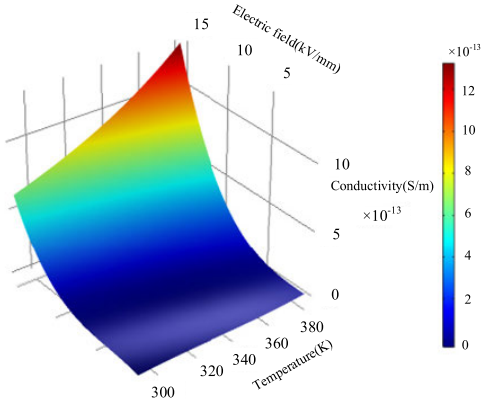

FIGURE 3. Conductivity plane of oil-immersed PB.

than $1e^{-14}$ S/m while the changed scope of temperature is 10K approximately.

C. ELECTRIC-STRESS DEPENDENCE OF OIL

Obviously, transformer-board conductivity varies with field intensity in exponential manner, whereas oil conductivity changes with electric field in the form of a saddle-like curve. The obtained experimental results differ from the previous assumption, which affects the insulation capability, because the electric field component for E <2 kV/mm is dominate in the transient electric field of converter transformer. Fig. 4 shows the probabilistic density of electric filed at some moments.

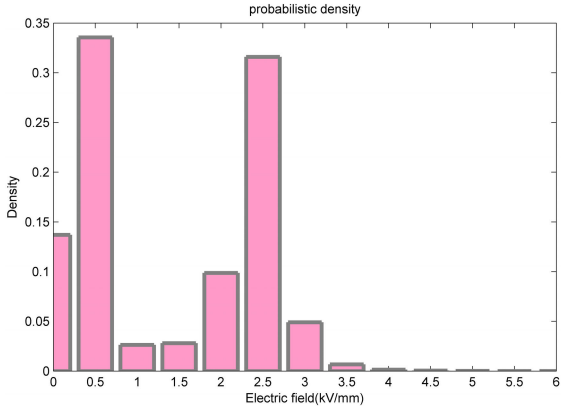

FIGURE 4. Probabilistic density of the electric field.

The wave tendency of the transformer oil conductivity is caused by two reasons. First, the production and dissipation of free ion directly affect oil conductivity. If the dissipation rate is larger than the producing rate, then the density of oil ions decreases, thereby decreasing oil conductivity. The main reason is that the external electric field breaks the original dynamic balance of dissociation and recombination and make oil approach to electrolyze completely. Equation (2) demonstrates the effect of applied electric field on dissociation and recombination, which influences the conductivity [14].

$$\sigma\,(E) = (K_+ + K_-)_0\, e_0 \left(k_D\,(E) \big/ k_R\,(E)\right)^{1/2} \tag{2}$$

where σ is the conductivity, E is the electric field, and k_D, k_R are the coefficients of dissociation and recombination, respectively.

Second, when the number of produced ions becomes larger than that of dissipated ions, oil conductivity would increase. The effect of Wien and Onsager theory performs an important role in conductivity when the electric field is maintained in a high level; thus, oil conductivity increases with the influence of charge injection. Equation (3) depicts the relationship between conductivity and applied electric field with a charge injection [15], [16].

$$\sigma\,(E) = \sigma_0 \left(k_{es} F\,(b) \big/ K_R\,(E)\right)^{1/2} \tag{3}$$

where σ is the conductivity, E is the electric field, $F(b)$ is the Bessel equation, and $k_{\rm es}$ is the coefficient. The changing conductivity is the coupling parameter to be utilized in the electric sub-model.

III. MULTI-PHYSICS FIELDS MODEL OF CONVERTER TRANSFORMER

A. COMPOUND AC-DC VOLTAGE

The exciting voltage [17] for the calculating electric field is obtained through the built HVDC transmission system model by PSCAD, as shown in Fig.5. The voltage source of line winding is a sinusoidal function, whereas the hybrid voltage exciting valve winding includes direct current component, fundamental frequency alternating current and higher harmonic component. Fig. 6 presents the voltage curves.

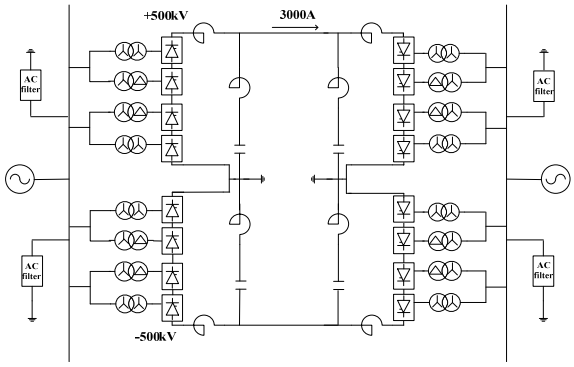

FIGURE 5. HVDC transmission system mode.

Fourier series analysis is applied to decompose compound AC-DC voltage. Fig. 7 depicts the amplitudes of every harmonic. The voltage is composed of DC current, fundamental frequency alternating current and higher harmonic component. In this study, an Y0- Δ converter transformer in a HVDC system is selected to investigate the nonlinear coupling phenomena.

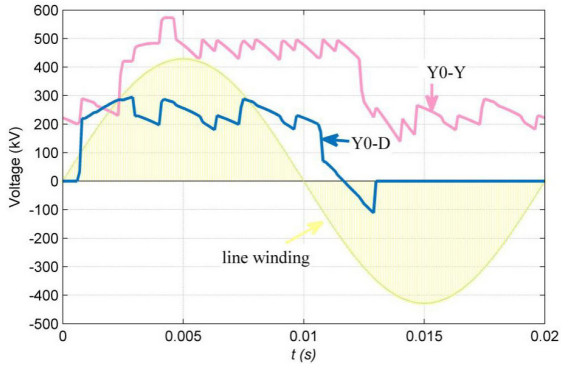

FIGURE 6. Compound AC-DC voltage curve.

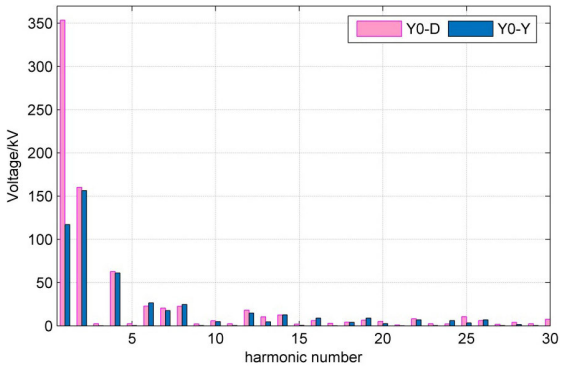

FIGURE 7. Spectrum analysis of voltage source.

B. ELECTROMAGNETIC-FLOW-THERMAL COUPLING

Heat sources include iron [18] and winding losses, which are calculated within the consideration of high-order harmonics. The magnetic flux density can be calculated on the basis of Maxwell equations, and the magnetic vector potential vector can be described as follows:

$$\frac{\partial}{\partial r}\nu\left(\frac{1}{r}\frac{\partial(r\boldsymbol{A}_\alpha)}{\partial r}\right)+\frac{\partial}{\partial z}\nu\left(\frac{1}{r}\frac{\partial(r\boldsymbol{A}_\alpha)}{\partial z}\right)=j\omega\sigma(r\boldsymbol{A}_\alpha)-\boldsymbol{J}_s \tag{4}$$

where $\boldsymbol{A}$ is the magnetic vector potential;ν and σ are the reluctivity and conductivity, respectively; $\boldsymbol{J}_s$ represents the source current density of winding; and z and r stand for the axial and radial directions, respectively.

The type of silicon steel sheets is 30RG120, and the influence of frequency is considered in calculating iron losses. Firstly, the B-P and B-H curves should be measured at 50 Hz on the basis of the selected silicon steel sheets. After the maximum magnetic flux density of every element B_m is obtained, mass loss P of every element, excited by fundamental frequency AC, is obtained by the B-P curve.

$$P=\rho h_j\sum_{i=1}^{N}P^{(i)}(B_m^{(i)})S_i \tag{5}$$

where P is the iron loss of every element at a fundamental frequency, ρ is the density, h_j is the thickness of the iron core in the jst class, N is the total number of elements, and S_i is the area of every element.

Considering the influence of high-order harmonics, as analyzed in Fig. 7, the losses have been studied by using loss separation method. The core losses [19] mainly include the hysteresis, eddy current, and additional losses, which can be expressed as:

$$P=K_h f^\alpha B_m^\beta+K_e\,(fB_m)^2 \tag{6}$$

where the first item on the right is the sum of the hysteresis and excess losses, the second item is the eddy current loss, f is the frequency, and B_m is the maximum magnetic flux density. K_h, K_e, α and β are the constants obtained from losses curve.

Winding losses [20] consist of ohmic and eddy losses as Eq.(7). Ohmic losses are dominant, which can be affected by high-order harmonics. The coefficient is the ratio of currents, as expressed in Eq.(8).

$$\begin{aligned}P_w&=P_\Omega+P_{eddy}\\&=\sum_{e=1}^{N}\frac{N^2I^2}{S^2\sigma}S_e+\frac{1}{24}\sigma(\omega dB)^2S_e\end{aligned} \tag{7}$$

where P_W is the winding loss; I and N are the current and number of turns, respectively; S is the area of the winding model; d is the wire size; ω is the angular frequency; B is the magnetic flux density in one element; and S_e is the area of one element.

$$P_\Omega^{'}=\frac{I_h}{I_f}P_\Omega \tag{8}$$

where P_Ω is the ohmic loss at a fundamental frequency, I_f is the fundamental current, and I_h is the current of the h^{th} high-order harmonics.

Through the thermal convection of transformer oil, winding losses are transferred to an oil tank, and the temperature is increased. The Mach number of transformers is small, and the steady-state mass conservation equation [21] of incompressible flow is as follows:

$$\frac{\partial(\rho u)}{\partial z}+\frac{1}{r}\frac{\partial(\rho rv)}{\partial r}=0 \tag{9}$$

The momentum conservation equations are as follows:

$$\begin{aligned}&\frac{\partial(\rho uu)}{\partial z}+\frac{\partial(\rho vu)}{\partial r}\\&\quad=f_z-\frac{\partial p}{\partial z}+\frac{\partial}{\partial z}(\mu\frac{\partial u}{\partial z})+\frac{1}{r}\frac{\partial}{\partial r}(\mu r\frac{\partial u}{\partial r})\end{aligned} \tag{10}$$

$$\begin{aligned}&\frac{\partial(\rho uv)}{\partial z}+\frac{\partial(\rho vv)}{\partial r}\\&\quad=f_r-\frac{\partial p}{\partial r}+\frac{\partial}{\partial z}(\mu\frac{\partial v}{\partial z})+\frac{1}{r}\frac{\partial}{\partial r}(\mu r\frac{\partial v}{\partial r})\end{aligned} \tag{11}$$

The energy conservation equation is shown as follow:

$$\begin{aligned}&\frac{\partial(\rho uc_pT)}{\partial z}+\frac{\partial(\rho vc_pT)}{\partial r}\\&\quad=s_T+\frac{\partial}{\partial z}(\lambda\frac{\partial T}{\partial z})+\frac{1}{r}\frac{\partial}{\partial r}(\lambda r\frac{\partial v}{\partial r})\end{aligned} \tag{12}$$

where z and r are the axial and radial directions, respectively; u and v are the axial and radial velocities, respectively; and f_z and f_r are the axial and radial external force densities, respectively, which are caused by gravity in this study. ρ is the density, μ is the dynamic viscosity, λ is the thermal conductivity, and c_p is the heat capacity at a constant pressure. S_T is the heat source, including the iron and winding losses introduced previously. In addition, the relationship between kinematic viscosity and temperature is also counted, since the kinematic viscosity decreases with temperature [5].

The ambient temperature is set as 298 K and a defined heat transfer coefficient is applied to the oil tank to simulate the heat convection of air, which can be described as follows [22]:

$$-\lambda\frac{\partial T}{\partial n} = h(T - T_{amb}) \tag{13}$$

where n is the normal direction, h is the convective heat transfer coefficient, and T_{amb} is the ambient temperature.

C. NONLINEAR THERMAL-ELECTRIC COUPLING

In the nonlinear thermal-electric coupling calculation process, the mapped temperature data to electric field calculation model should be utilized, and the electric-stress dependence of the conductivity should be considerable, as measured in Part II. The electric quasi-static field can be measured as follows:

$$\begin{cases} \nabla\cdot(\varepsilon\partial/\partial t + g(T,E))\nabla\varphi = 0, \quad \varphi\in\Omega \\ \varphi|_{\Gamma_1} = u(t) \\ \dfrac{\partial\varphi}{\partial n}|_{\Gamma_2} = \psi(t) \\ \varphi|_{t=0} = \varphi(0) \end{cases} \tag{14}$$

where Ω is computational region and φ is potential; ε is dielectric constant, and g is conductivity which is the function of temperature and field intensity here. Γ_1 and Γ_2 are Dirichlet boundary condition and Neumann boundary condition respectively. And t is time, E is electric field.

D. TEMPERATURE IN SUB-MODEL

The transformer oil flows from the inlet at the bottom to the outlet at the top; thus, the thermal-velocity coupling model is adopted to analyze the temperature distribution of the entire model. While the middle of winding is grounded in the electric research, the sub-model is adopted with the symmetry axis being the Neumann boundary condition. Moreover, the best fitting grids between the temperature and electric fields have different shapes and sizes, and fine grids at regions with large temperature gradient should be generated [23]. Therefore, the fast mapping method is applied to interpolate temperature results into the sub-model, which could call these temperature data in thermal-electric coupling calculation [24].

As shown in Fig. 8, (x, y) is the coordinate of node D in the sub-model, and the temperature date of node D' can be

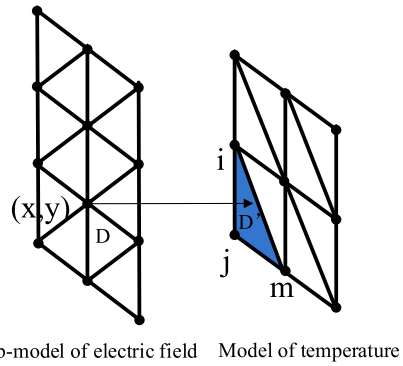

FIGURE 8. Schematic of the fast mapping method.

obtained by a shape function.

$$\begin{cases} x = x_iN_i + x_jN_j + x_kN_k \\ y = y_iN_i + y_jN_j + y_kN_k \end{cases} \tag{15}$$

The shape function in one element has the following relationship:

$$N_i + N_j + N_k = 1 \tag{16}$$

Substituting Eq. (15) into Eq. (14) obtains Eq. (16).

$$\begin{cases} (x_i - x_k)N_i + (x_j - x_k)N_j = x_k - x \\ (y_i - y_k)N_i + (y_j - y_k)N_j = y_k - y \end{cases} \tag{17}$$

If the shape function $N_m(m = i, j, k)$ is less than 1, then the temperature data of the sub-model can be described:

$$T_D = T_{D'i}N_i + T_{D'j}N_j + T_{D'k}N_k \tag{18}$$

where $T_{D'i}$, $T_{D'j}$, and $T_{D'k}$ are node data of the temperature field. Fig. 9 shows the model structures and mesh conditions of two physical fields.

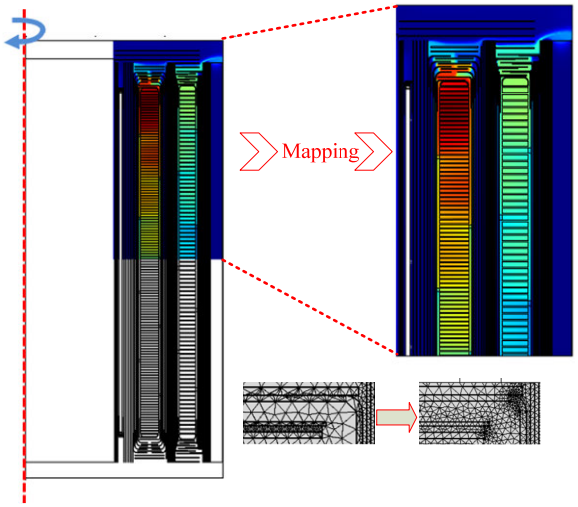

FIGURE 9. Temperature field of meshing.

IV. MATHEMATICAL MODEL

A. CALCULATION PROCESSES

Fig. 10 concludes the entire calculation processes. Before the coupling analysis, the time constants of the transformer oil and PB insulation system are relatively large, generally reaching thousands of seconds, whereas the period of excited voltage is only 0.02 s. Therefore, temperature can be thought as unchanged in electric analysis. Iron and winding losses with high-order harmonics are studied in the first step. In the temperature analysis process, the inlet velocity and outlet pressure are set as boundary conditions, and the losses are generated heat sources. Then, thermal-velocity coupling calculation is applied to the entire model. Finally, the nonlinear thermal-electric coupling is studied after the non-uniform temperature field mapped partly to an electric sub-model by interpolation. Conductivity affected by thermal-electric condition is seen as coupling parameter, which is the function of temperature and field intensity in electric field calculation. The whole process is done by finite element method and iteration method.

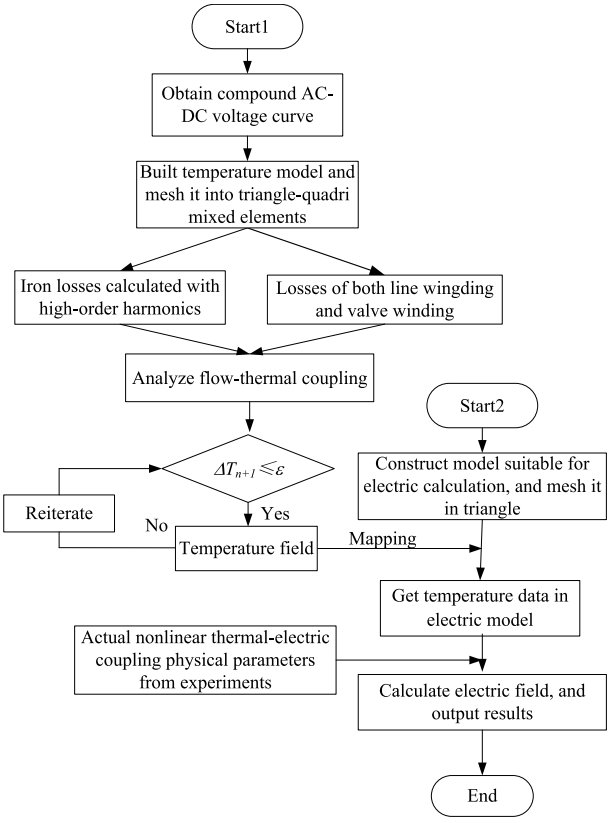

FIGURE 10. Process of thermal-electric coupling calculation.

B. ENTIRE MODEL IN TEMPERATURE FIELD

Fig. 11 shows the computational model, a quarter of a converter ±500 kV transformer. Multi-level meshing has been adopted to the critical components, and fine meshing is processed rather than other layers, such as windings and iron core. All grids are close to the ideal shape, and fine grids

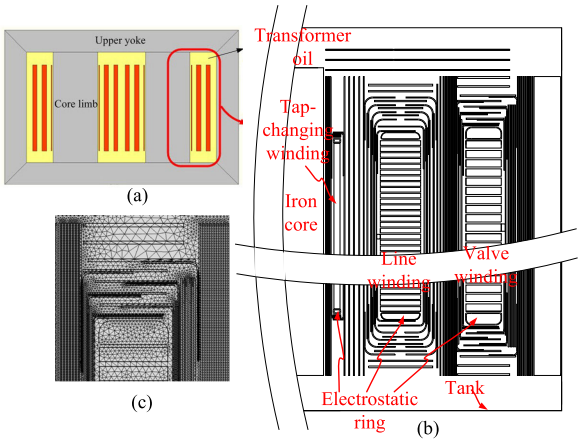

FIGURE 11. Model of electromagnetic-flow-thermal analysis.(a) Model of converter transformer. (b) Entire model of the thermal analysis. (c) Meshing condition.

at regions with large temperature gradient are generated. The total number of nodes is 157652, the total number of body elements is 315181, and the average element quality measured by skew is 0.65, which meets the criteria of meshing quality. A grid independent study is conducted on grid sizes of 0.12, 0.15, and 0.19 million nodes. The maximum winding temperature changes by less than 0.2% compared with the result with the finest grid, and the location of the hot spot is always in the 7th disc. Thus, the grid size of 0.15 million nodes is considered sufficient and used in all present simulations.

Fig. 12 shows the sub-model with the Neumann boundary condition of electric field due to grounded middle turns of winding. To analyze the hybrid electric field, the valve winding stands compound AC-DC voltage, as displayed in Fig. 7, and the fundamental sinusoidal voltage excites the line winding. Moreover, AB and BC are the walls of oil tank, whereas

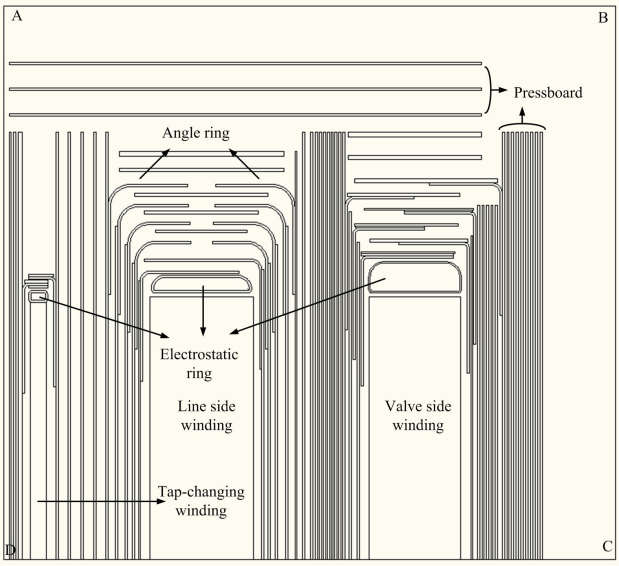

FIGURE 12. Sub-model of the electric field.

the AD line refers to one boundary of the iron core; these three lines are grounded [25].

V. EFFECT OF SADDLE-LIKE ELECTRIC-STRESS DEPENDENCE

A. COMPARISON WITH EXPONENTIAL VARIATION

The electric-stress dependence of oil conductivity varies with the voltage in exponential manner. By measuring the physical parameter, a saddle-like tendency occurs between the field intensity and conductivity, as shown in Section II. To study the effect of saddle-like electric-stress dependence, two types of conductivity relationship are applied and compared. In Fig. 13, the fitting relationship of experimental data has saddle-like changing tendency as the black curve shows. Another traditional changing tends in exponential polynomial manner as red curve shows. To study the effect of saddle-like type explicitly, data after 2kV/mm are approximately equal in two curves to avoid other interference terms.

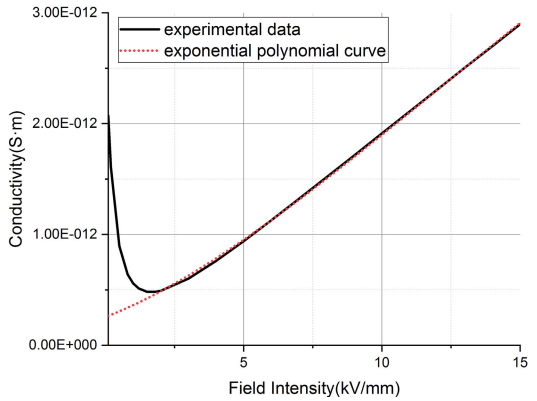

FIGURE 13. Comparison of conductivity curves under two conditions.

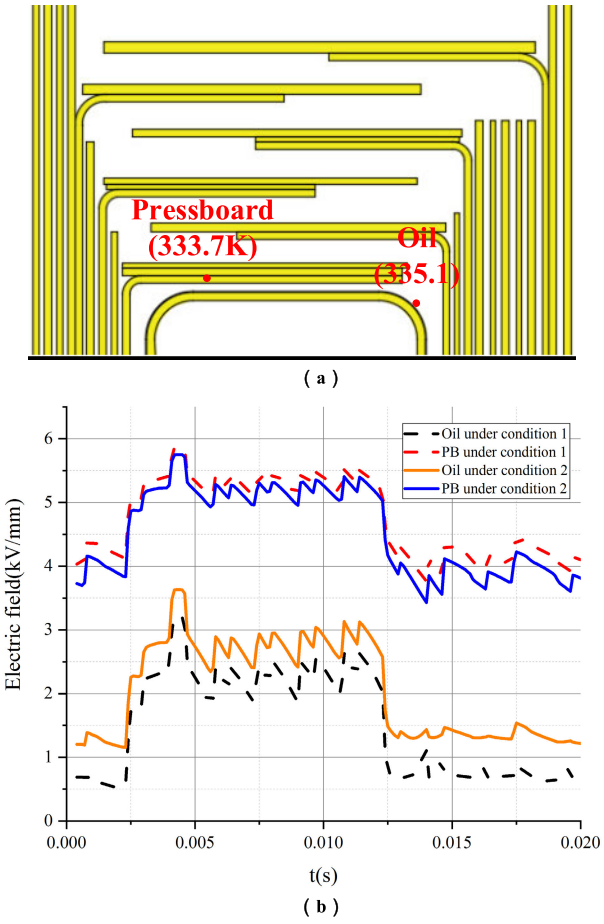

FIGURE 14. Electric variation of oil sampling point. (a) Location of sampling point. (b) Changing curve under two conditions.

Fig. 14(a) shows the location and temperature of sampling points, Fig. 14(b) displays the changing curve of oil and PB under two different conditions. Two numerical simulations are performed on the basis of the properties of oil conductivity: condition 1, stereotype manner in exponential fitting function; condition 2, saddle-like electric-stress dependence (as experimented in Part II). The field intensity of PB sampling points stays unchanged with the consideration of saddle-like properties, but the field intensity of the oil sampling point increases gradually, even more than 0.5 kV/mm. The rising variation of field intensity indicates that the saddle-like electric-stress dependence may lead to a relatively safe point to face the potential hazard and even cause insulation failure. Hence, practical saddle-like properties must be considered in insulation design.

B. SADDLE-LIKE CHANGE IN THERMAL-ELECTRIC COUPLING

To count the influence of temperature, uneven loss distributions are studied as Eq.(4–8), and thermal-velocity coupling is calculated as Eq. (9–12) by using finite element method.

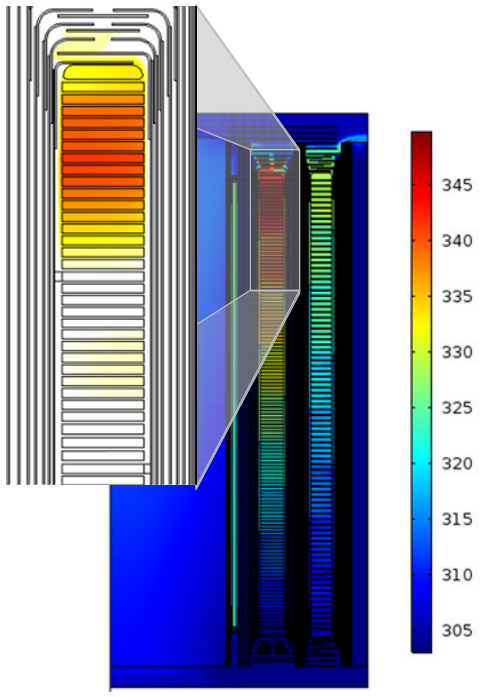

FIGURE 15. Temperature distribution and location of the hot spot.

Fig. 15 shows the temperature contour of converter transformer, and the enlarged figure on the left shows a high temperature of over 342 K to observe the location of the hot spot. It's obvious that temperature differences exist markedly in the insulation system, and the temperature gradient of some pressboards can be up to 6 K/mm, and these thermal data are listed in Table 1. Therefore, the nonlinear thermal-electric coupling characteristic should be counted in electric calculation.

TABLE 1. Temperature of insulating materials.

Item	Transformer oil	Oil-immersed PB
T_{avg} (K)	309.0	307.2
T_{max} (K)	349.8	345.0
T_{max}-T_{amb} (K)	51.8	47.0

Based on the steady nonuniform temperature distribution in Fig.15, Fig. 16 shows that the potential contours at 0.005 and 0.015 s under two conditions. In considering saddle-like properties, the pressboard stands at a high field intensity, and the maximum value is close to 9 kV/mm at 0.015s. Additionally, the electric distribution of the transformer oil becomes uneven, especially at the end of horizontal pressboard.

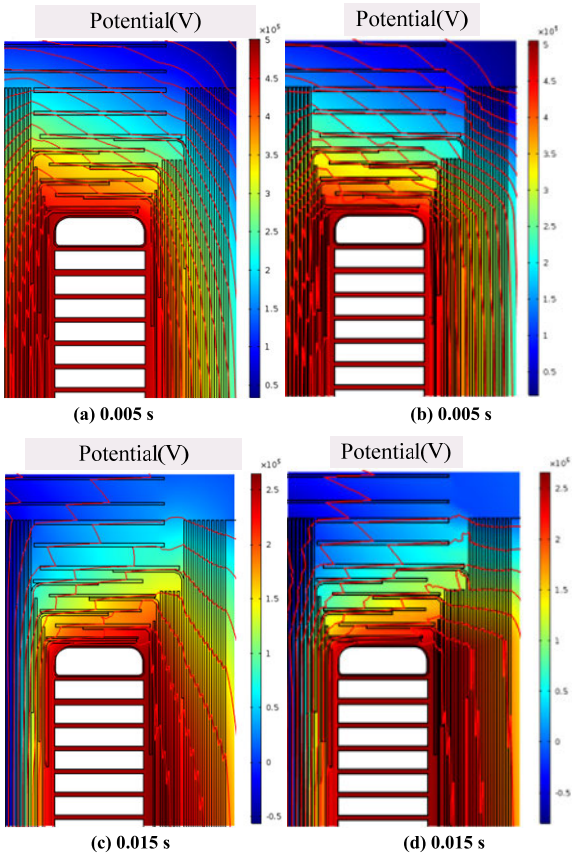

FIGURE 16. Electric field at three quarters of the cycle. (a)(c) Traditional exponential manner. (b)(d) Saddle-like thermal-electric changing relationship.

Fig. 17 displays the field intensity of sampling points, as located in Fig. 14(a). The difference between conditions (condition 2 considers saddle-like change) becomes more obvious due to non-uniform temperature distribution. The pressboard field intensity with saddle-like thermal-electric properties jumps by 1.3 kV/mm compared with that under condition 1, whereas the oil electric filed increases by more than 1.6kV/mm. This changing trend is similar to that in Fig. 14(b).

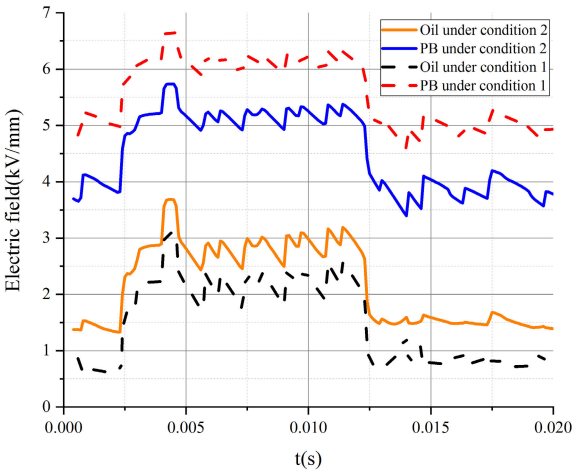

FIGURE 17. Electric variation of PB sampling point under two manners.

Markedly, the insulation state of oil sampling point is more severe within the influence of saddle-like properties, and the maximum electric field is an important factor for evaluating the insulation capability of the transformer oil. Fig. 18 depicts the maximum value at every moment. The changing tendency is similar to a sinusoidal curve, which indicates that the oil point with maximum value is next to the line winding. However, the variation affected by saddle-like properties is

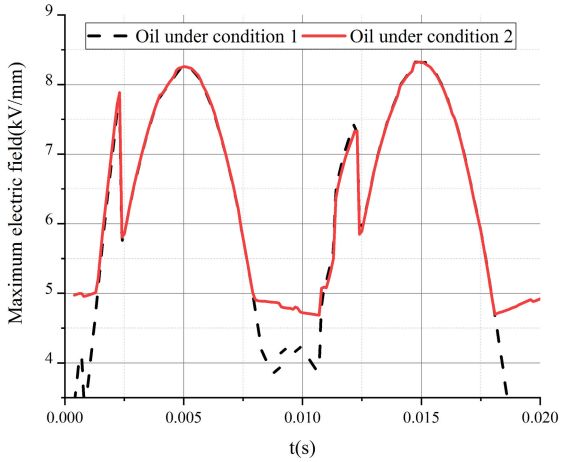

FIGURE 18. Maximum value of transformer oil in one period.

not evident. The reason is that the electric field distribution near the line winding depends on the dielectric constant rather than conductivity.

VI. CONCLUSION

Based on the found saddle-like electric-stress dependence of insulation system in converter transformer, the thermal-electric coupling performance under compound AC-DC voltage is investigated, and some comparisons of different insulation material properties are also discussed. The obtained conclusions are summarized as follows:

(1) Three-electrode experimental system is constructed to test the conductance of transformer oil and oil-immersed pressboard. It is found that the electric-dependent conductivity of transformer oil shows a variation trend with saddle-shape.

(2) The voltage of valve winding has been simulated in HVDC transmission system, and the hybrid voltage is analyzed by spectrum analysis to study iron and winding losses with high-order harmonics. In addition, the non-uniform temperature indeed has great impact on the insulation ability through the built electromagnetic-thermal-velocity coupling model, and the highest temperature is 350 K, with temperature gradient is up to 6K/mm.

(3) The saddle-shape property has important impact on the electric field distribution. The field intensity of some points has changed and even increased by more than 1.6 kV/mm due to saddle-like change. The increase will cause additional points in the transformer to face the safety hazard, which may paralyze the normal operation.

REFERENCES

[1] G. Liu, C. Chi, Y. Jin, Y. Ma, L. Sun, L. Li, and Y. Sun, "Analysis of non-sinusoidal steady electric field of ±500 kV converter transformer," *Energy Power Eng.*, vol. 9, no. 4, pp. 53–62, 2017.

[2] T. Terakura, K. Takano, T. Yasuoka, S. Mori, O. Hosokawa, T. Iwabuchi, T. Chigiri, and S. Yamada, "Transient electric field analysis in consideration of the electric field dependence of resistivity in the converter transformer," *Elect. Eng. Jpn.*, vol. 198, no. 1, pp. 3–11, 2017.

[3] H. Li, L. Zhong, Q. Yu, S. Mori, and S. Yamada, "The resistivity of oil and oil-impregnated pressboard varies with temperature and electric field strength," *IEEE Trans. Dielectr. Electr. Insul.*, vol. 21, no. 4, pp. 1851–1856, Aug. 2014.

[4] C. Gao, B. Qi, S. Liu, O. Liu, and C. Li, "Research on the variation of transformer pressboard's resistivity and permittivity with temperature and moisture," presented at the Elect. Insul. Conf., Birmingham, U.K., 2017.

[5] G. Liu, C. Chi, L. Li, Y. Jin, Y. Ma, and L. Sun, "Influence of non-uniform temperature on transient electric field for ±500 kV converter transformer under polarity reversal voltage," *Int. J. Appl. Electromagn. Mech.*, vol. 56, no. 3, pp. 445–459, 2018. doi: 10.3233/JAE-170072.

[6] Y. Xie, L. Li, and Y. Song, "Multi-Physical field coupled method for temperature rise of winding in oil-immersed power transformer," *Proc. CSEE*, vol. 6, no. 21, pp. 5957–5965, 2016.

[7] L. Li, Y. Xie, G. Liu, and S. Wang, "Influencing factor analysis for disc-type winding temperature rise of oil-immersed power transformer," *Electr. Power Automat. Equip.*, vol. 36, no. 12, pp. 83–88, 2016.

[8] L. Gang *et al.*, "Influence of non-uniform temperature on the 2D non-sinusoidal steady AC-DC compound electric field in ±500 kV converter transformer," *Proc. CSEE*, vol. 38, no. 8, pp. 2521–2529, 2018.

[9] F. Torriano, P. Picher, and M. Chaaban, "Numerical investigation of 3D flow and thermal effects in a disc-type transformer winding," *Appl. Therm. Eng.*, vol. 40, pp. 121–131, Jul. 2012.

[10] CIGRE Joint Working Group. (2016). *HVDC Transformer Insulation: Oil Conductivity*. [Online]. Available: http://www.ecigre.org/publication/646-hvdc-transformerinsulation-oil-conductivity

[11] X. Zhengyu *et al.*, "Real time test system and method of conduction characteristics of oil-paper insulation," *High Voltage Eng.*, vol. 41, no. 1, pp. 231–236, 2015.

[12] *IEEE Criteria for Methods of Test for Volume Resistivity and Surface Resistivity of Solid Electrical Insulating Materials*, IEEE Standard 60093, 1980.

[13] *Standards Press of China, Test Method For Volume Resistivity and Surface Resistivity of Solid Insulating Materials*, Standard GB1410-2006, 2006.

[14] D. André, "Conduction and breakdown initiation in dielectric liquids," presented at the IEEE Int. Conf. Dielectr. Liquids, Trondheim, Norway, Jun. 2011.

[15] F. Pontiga and A. Castellanos, "A field-dependent injection-dissociation model for electrical conduction in nonpolar liquids," presented at the Ind. Appl. Society Meeting, Oct. 1994.

[16] A. Denat, B. Gosse, and J. P. Gosse, "Ion injections in hydrocarbons," *J. Electrostatics*, vol. 7, pp. 205–225, Aug. 1979.

[17] L. Gang, L. Lin, and Z. Xiaojun, "Analysis of nonlinear electric field of oil-paper insulation under AC-DC hybrid voltage by fixed point method combined with FEM in frequency domain," *Proc. CSEE*, vol. 32, no. 1, pp. 154–161, 2012.

[18] I. Žiger, B. Trkulja, and Ž. Štih, "Determination of core losses in open-core power voltage transformers," *IEEE Access*, vol. 6, pp. 29426–29435, 2018.

[19] Q. Cheng, Z. Zhang, and N. Xie, "Power losses analysis of the gasoline direct injector within different driven strategies," *Int. J. Appl. Electromagn. Mech.*, vol. 50, no. 3, pp. 379–394, 2016.

[20] Y. Li, D. Eerhemubayaer, Y. Jing, X. Sun, and S. Yang, "Calculation and control of stray losses in power transformer," *Int. J. Appl. Electromagn. Mech.*, vol. 39, nos. 1–4, pp. 835–841, 2012.

[21] X. Zhang, Z. Wang, Q. Liu, P. Jarman, and M. Negro, "Numerical investigation of oil flow and temperature distributions for ON transformer windings," *Appl. Therm. Eng.*, vol. 130, pp. 1–9, Feb. 2018.

[22] Y. Shiming and T. Wenquan, *Heat Transfer*. Beijing, China: Higher Education Press, (in Chinese), 2006.

[23] Y. Zhang, W. Qin, D. Liu, and G. Wu, "Non-matching meshes mapping method in coupled magnetic and thermal analysis of electromagnetic devices," *Trans. China Electrotech. Soc.*, vol. 31, no. 13, pp. 141–148, Jul. 2016.

[24] G. Liu, H. Zhang, C. Chi, L. Li, and H. Li, "Research on node data mapping algorithm for the 2D coupling electromagnetic-fluid-thermal fields," *Trans. China Electrotechnical Soc.*, vol. 33, no. 1, pp. 148–157, 2018.

[25] Z. Jing, *Supervision Technology of Converter Transformer*. Beijing, China: China Electric Power Press, 2016.

DUAN PAN received the Ph.D. degree from the School of Electrical Engineering, Chongqing University, Chongqing, China, in 2012. He is currently an Associate Professor with the School of Automation, Chongqing University of Posts and Telecommunications, Chongqing. His research interests include the reliability and economy of power systems and smart grid, the multi-physics coupling field calculation, and healthy detection of renewable devices.

GAO BING received the Ph.D. degree from the School of Electrical Engineering, Chongqing University, Chongqing, China, in 2016, where he is currently a Lecturer. His research interests include the reliability of power modules, the multi-physics coupling field calculation for power electronics, and the development of condition monitoring methods for power electronic converters.

CHI CHENG was born in Chongqing, China. She received the master's degree from the School of Electrical Engineering, North China Electric Power University, China, in 2018. She is currently pursuing the Ph.D. degree with the School of Electrical Engineering, Chongqing University, China. Her research interests include multi-physics coupling field calculation of electrical equipment and computational electromagnetic in high-voltage apparatus.

YANG FAN (M'11) received the Ph.D. degree from the School of Electrical Engineering, Chongqing University, China, in 2008, where he is currently a Professor of electrical engineering. He was a Visiting Scholar with Oklahoma State University, OK, USA, in 2012. His research interests include condition monitoring methods for electrical apparatus and the multi-physics coupling field calculation for renewable devices.

LUO PING was born in Guiyang, China. She is currently an Associate Professor with the School of Automation, Chongqing University of Posts and Telecommunications. Her research interest includes electric and electronic transmission and control.